ELSEVIER

International Journal of Mass Spectrometry 218 (2002) 87–101

International Journal of Mass Spectrometry

www.elsevier.com/locate/ijms

A selected ion flow tube (SIFT), study of the reactions of H_3O^+, NO^+ and $O_2{}^+$ ions with a series of alkenes; in support of SIFT-MS

Ann M. Diskin[a], Tianshu Wang[a], David Smith[a,*], Patrik Španěl[b]

[a] *School of Postgraduate Medicine, Centre for Science and Technology in Medicine, Keele University, Thornburrow Drive, Hartshill, Stoke on Trent ST4 7QB, UK*
[b] *V.Čermák Laboratory, J. Heyrovský Institute of Physical Chemistry, Academy of Sciences of the Czech Republic, Dolejškova 3, 182 23 Prague 8, Czech Republic*

Received 19 March 2002; accepted 15 April 2002

Abstract

We report the results of a detailed selected ion flow tube (SIFT) study at 300 K of the reactions of the 1-alkene and *trans*-2-alkene isomers of pentene, hexene, heptene, octene and nonene and 1-decene (all liquids at room temperature) with H_3O^+, NO^+ and $O_2{}^+$. All 33 reactions proceeded at the collisional rate under these SIFT conditions (helium carrier gas pressure of 0.7 Torr). The H_3O^+ reactions with both isomers of each alkene proceeded via exothermic proton transfer, which resulted in partial dissociation of the MH^+ product ions for the longer chain alkene molecules, M, the number of fragment ions depending on the chain length. However, the mechanisms of the NO^+ reactions were isomer specific, those involving the 1-alkenes proceeded via $NO^+\cdot M$ production (three-body association) followed by partial stabilisation and partial dissociation of the nascent adduct ion to several products, including ions of the kind $RHNO^+$ ($R = CH_3$, C_3H_5, C_4H_7, etc.), whilst those involving the *trans*-2-alkene isomers proceeded partially via charge (electron) transfer to give M^+ parent ions and via hydride ion (H^-) transfer giving $(M–H)^+$ ions. The $O_2{}^+$ reactions all proceeded via charge transfer to give M^+ ions together with multiple fragment ions. These $O_2{}^+$ SIFT data are compared and contrasted with the corresponding electron ionisation spectra (from the NIST database) for these alkenes. (Int J Mass Spectrom 218 (2002) 87–101) © 2002 Elsevier Science B.V. All rights reserved.

Keywords: SIFT; Alkenes; Proton transfer; Charge transfer; Association; Dissociation

1. Introduction

In recent years, we have developed the selected ion flow tube mass spectrometric technique (SIFT-MS), for the analysis of trace gases in air, breath and the headspace above liquids at the parts per billion (ppb) level [1,2]. Using this technique, accurate analysis can be accomplished in real time, giving immediate results, avoiding the need for pre-concentration of the trace volatile compounds from the air/breath samples [1–3]. We are now using SIFT-MS for various research programmes. These include breath analysis and urine headspace analysis for clinical diagnosis and therapeutic monitoring [4], especially for those suffering from renal failure [5] and cancer [6], in animal husbandry [7,8] and, most recently, to study the emission of molecules from various cell cultures [9].

SIFT-MS involves the chemical ionisation of the trace gases in the air sample to be analysed by selected precursor ions, viz., H_3O^+, NO^+ and $O_2{}^+$

---

* Corresponding author. E-mail: d.smith@bemp.keele.ac.uk

PII S1387-3806(02)00662-0

[10] (see later). Recognition of the products of these reactions allows the trace gases to be identified and quantified [11,12]. The essential point is that the reactions of a large number of organic and inorganic vapours and gases with H_3O^+, NO^+ and $O_2{}^+$ ions have had to be studied to provide the kinetics database that is needed to perform the variety of studies mentioned previously. The current SIFT-MS database consists of the rate coefficients and product ions of hundreds of such reaction as studied using the SIFT method, which provides the kinetic data at thermal energies, as required [13–23]. This kinetics database is continuously being expanded in response to the demands of the different SIFT-MS applications. Recently, we embarked on a study of the pollutant gases emitted by petrol and diesel vehicle engines [24]. As is generally known, a cocktail of organic and inorganic species is emitted by these engines [25], including aliphatic and aromatic hydrocarbons, aldehydes, ketones, alcohols and the oxides of nitrogen [25]. Our database is able to cope with most of these compounds, thus allowing on-line real time analyses of them. This has been helped by our very recent survey of the reactions of aldehydes [23] and our earlier survey of the reactions of alkanes and aromatic hydrocarbons [20]. However, our database was deficient in the reactions of alkenes, several of which appear above petrol and diesel fuel and also in the exhausts of the vehicle engines [24]. Little previous work is available on the reactions of the H_3O^+, NO^+ and $O_2{}^+$ ions with alkenes with the exception of the isomers 1-pentene and 2-methyl-2-butene included in our hydrocarbon survey [20] and the recent study of the NO^+ reactions with butene isomers [26]. We have therefore carried out a detailed SIFT study of the reactions of the 1-alkene and *trans*-2-alkene isomers of pentene, hexene, heptene, octene and nonene and also 1-decene (all liquids at room temperature) with H_3O^+, NO^+ and $O_2{}^+$. This study is primarily in support of our SIFT-MS studies of vehicle exhaust gases, but as we will see it has produced a good deal of interesting, fundamental data on these alkene reactions. The alkenes were obtained from Sigma–Aldrich and they have the following purities: (1-pentene 99%, *trans*-2-pentene 99%, 1-hexene 97%, *trans*-2-hexene 97%, 1-heptene 97%, *trans*-2-heptene 99%, 1-octene 98%, *trans*-2-octene 97%, 1-nonene 98%, *trans*-2-nonene 99% and 1-decene 94%). Unfortunately, the *trans*-2-decene was not available from our suppliers.

2. Experimental

The transportable SIFT instrument (TSIFT) Mk.1, at Keele University was used for the present experiments. The SIFT is a standard technique for the study of ion–molecule reactions at thermal energies that has been described in numerous research papers and review articles (see, as examples, [2,27]). In the TSIFT instrument, H_3O^+, NO^+ and $O_2{}^+$ ions are created in a microwave discharge through a mixture of water vapour and air (at a total pressure of about 0.2 Torr). The ions are then selected and injected into helium carrier gas (at a pressure of about 0.7 Torr) via a quadrupole mass filter operated at a suitable resolution to optimise the transmitted ion current. Alternatively, the three ions can be injected simultaneously in order to determine relative rate coefficients for their reactions with particular neutral species (see below). The ions are convected along the flow tube by the carrier gas and, as usual, are sampled downstream via a pinhole/quadrupole mass spectrometer and detected and counted by a channeltron/amplifier/pulse counting system connected to a computer.

In a conventional SIFT study of the rate coefficients and ion products of reactions, the reactant gases are flowed into the carrier gas/precursor ion swarm at a measured and controlled rate. Then the count rates of the reactant ion (in this study H_3O^+, NO^+, $O_2{}^+$) and the products ions are determined as a function of the reactant gas flow rate. From these data the rate coefficient and the product ion distribution (ratio) are obtained by a standard procedure [27]. This is usually a simple procedure for permanent reactant gases, because calibrated mass flow meters and flow controllers can be used. These can also be used for the neat vapours of some organic liquids if the calibration constant for the vapour for the particular flow meter is known; if not, a known weak mixture of the vapour in an inert gas (e.g., helium, argon or nitrogen) can be used. However, because of the "sticky" nature of some of these alkenes and the scarcity of information on their physical properties, this procedure is not useful for these compounds. So the approach we take to the determination of the rate coefficients, *k*, and ion product distributions for the reactions is essentially identical to that taken for all our previous studies of the reactions of several other classes of liquid organic compounds [13–23]. This procedure is described in detail in our alcohols paper [13] and outlined in several subsequent papers [14–23], so only a brief outline of the method is required here and it is as follows.

We are able to assume that the *k* for the H_3O^+ reactions proceed gas kinetically with rate coefficient, k_c, because the proton affinities (PA), of the alkenes included in this study are expected to exceed the PA of the H_2O molecule which is 696 kJ/mol. (The PA of most of these alkenes are not known [28], but the PA of 1-propene (C_3H_6) is 751 kJ/mol, that of *trans*-2-butene (C_4H_8) is 747 kJ/mol and that of 1-hexene (C_6H_{12}) is 805 kJ/mol). Then, as for most all exothermic proton transfer reactions, the $k = k_c$ [29]. As we will see, the experimental evidence supports our expectation. So the *k* for the H_3O^+/alkene reactions need not be measured; rather a value of k_c can be adopted [13]. The k_c can be calculated [30] if the polarisabilities and dipole moments of the reactant molecules are known [31] or can be estimated. For these alkenes we have had to estimate the polarisabilities and some of the dipole moments by a procedure that we have used previously that involves comparison and extrapolation from those of similar compounds [20]. However, it cannot be assumed that the NO^+ and $O_2{}^+$ reactions proceed at the gas kinetic rate, because it is known that the reaction processes involved (e.g., charge transfer and hydride ion transfer sometimes proceed more slowly than the gas kinetic rate [32,33]). So the corresponding *k* for the NO^+ and $O_2{}^+$ reactions with each particular alkene are obtained from the *relative decay rates* of all three reactant ions (H_3O^+, NO^+ and $O_2{}^+$) as they are *simultaneously* injected into the helium carrier gas as a measured flow rate of a weak mixture of the alkene in relatively dry cylinder air is introduced simultaneously into the helium carrier gas (along heated flow lines to prevent condensation). A typical set of decay curves is shown in Fig. 1. Note that in this procedure the absolute flow rates of the alkene/air mixture are not required. These experimentally derived *k* values are listed in Table 1 and their absolute values are subject to an uncertainty of ±25% whilst their relative values are accurate to ±15%.

The identity of the product ions and their percentages for these reactions were obtained in the following way. A small amount of the alkene/air mixture, sufficient to reduce the reactant ion count rate by no more than a few percent, was introduced into the carrier gas. The downstream analytical mass spectrometer was then scanned several times over a predetermined range of mass-to-charge ratio, *m*/*z*, to record all the reactant and product ion count rates and to form a clear spectrum as is exemplified in Fig. 2. The percentage product ion distribution was simply obtained from the individual product ion count rates. This procedure was repeated for different concentrations of the alkene in the carrier gas to ensure that secondary reactions were not significantly modifying the ion product distributions. Further to this, spectral scans were also obtained at different resolutions of the quadrupole mass spectrometer to investigate any influence of mass discrimination against the larger product ions. The phenomena of differential diffusion of ions and mass discrimination have been thoroughly investigated for this TSIFT instrument and reported in detail [12].

It is important to note that a fraction (typically 10–15%) of the injected NO^+ and $O_2{}^+$ reactant ions are in electronically (and probably vibrationally) excited states prior to their entry to the flow tube and that these excited ions can persist in the helium carrier gas [34]. This excitation is partially quenched by the air that transports the reactant alkenes into the carrier gas, but to ensure total quenching we introduce a greater amount of dry cylinder air into the helium via another entry port. All these measurements were carried out in helium carrier gas at a pressure of 0.7 Torr at room temperature.

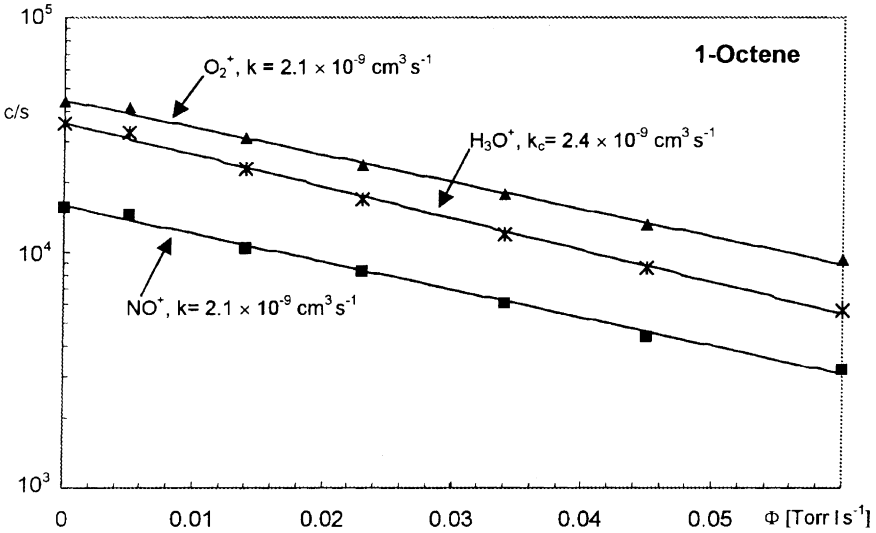

Fig. 1. Sample semilogarithmic plots of the count rates (c/s) of H_3O^+, NO^+ and $O_2{}^+$ ions as a dilute mixture of 1-octene in dry air flow rate, ϕ (Torr l/s) is introduced into the helium carrier gas of the SIFT. k_c is the calculated collisional rate coefficient for the H_3O^+ reaction with 1-octene (C_8H_{16}). The rate coefficients, k, for the NO^+ and $O_2{}^+$ reactions are obtained from the relative slopes of the decay plots (see Section 2).

To determine which of the product ions of these alkene reactions form hydrates, each experiment was repeated with a sufficient amount of humid laboratory air (about 1% water content) and much more humid breath (about 6% water content) entering the carrier gas. This immediately resulted in the partial conversion of reactant H_3O^+ ions to the $H_3O^+(H_2O)_{1,2,3}$ hydrates (the concentration of H_2O molecules can be

Table 1
Rate coefficients for the reactions of H_3O^+, NO^+ and $O_2{}^+$ with the alkenes indicated

Molecule	m (Da)	α ($\times 10^{-24}$ cm^3)	μ (Debye)	k_c (H_3O^+) ($\times 10^{-9}$ cm^3/s)	k, k_c (NO^+) ($\times 10^{-9}$ cm^3/s)	k, k_c ($O_2{}^+$) ($\times 10^{-9}$ cm^3/s)
1-Pentene	70	*9.5 ± 0.5*	*0.4 ± 0.05*	[2.0]	1.7 [1.7]	1.7 [1.6]
Trans-2-pentene	70	*9.5 ± 0.5*	0.050 ± 0.01	[1.9]	1.8 [1.6]	1.7 [1.6]
1-Hexene	84	*11.5 ± 0.5*	*0.4 ± 0.05*	[2.1]	1.8 [1.8]	1.8 [1.7]
Trans-2-hexene	84	*11.5 ± 0.5*	0.049 ± 0.01	[2.0]	1.9 [1.7]	1.8 [1.7]
1-Heptene	98	*13.5 ± 0.5*	*0.4 ± 0.05*	[2.3]	2.0 [1.9]	2.0 [1.8]
Trans-2-heptene	98	*13.5 ± 0.5*	0.055 ± 0.01	[2.2]	2.0 [1.8]	1.9 [1.8]
1-Octene	112	*15.5 ± 0.5*	*0.4 ± 0.05*	[2.4]	2.1 [2.0]	2.1 [1.9]
Trans-2-octene	112	*15.5 ± 0.5*	0.067 ± 0.01	[2.3]	2.1 [1.9]	2.1 [1.9]
1-Nonene	126	*17.5 ± 1.0*	*0.4 ± 0.05*	[2.5]	2.3 [2.1]	2.1 [2.0]
Trans-2-nonene	126	*17.5 ± 1.0*	*0.08 ± 0.01*	[2.4]	2.1 [2.0]	2.1 [2.0]
1-Decene	140	*19.5 ± 1.0*	*0.4 ± 0.05*	[2.6]	2.1 [2.2]	2.1 [2.1]

Molecular weights, m (Da), polarisabilities, α ($\times 10^{-24}$ cm^3) and permanent dipole moments, μ (Debye). The values of μ are known for some of the compounds included in this study and are shown in regular type (taken from [31,44]). For the remaining compounds we have estimated their α and μ (shown in italics) by adopting the values of similar unsaturated aliphatic molecules. Then the collisional rate coefficients, k_c, for all reactions have been calculated using the parameterised trajectory formulation of Su and Chesnavich [30] and are given in square brackets. On the assumption that all the H_3O^+ reactions proceed at the respective collisional rates, the rate coefficients, k, for the NO^+ and $O_2{}^+$ reactions have been experimentally derived by the procedure described in Section 2. The estimated absolute and relative uncertainties in these calculated rate coefficients are ±25 and ±15%, respectively. The k and k_c are given in units of $\times 10^{-9}$ cm^3/s.

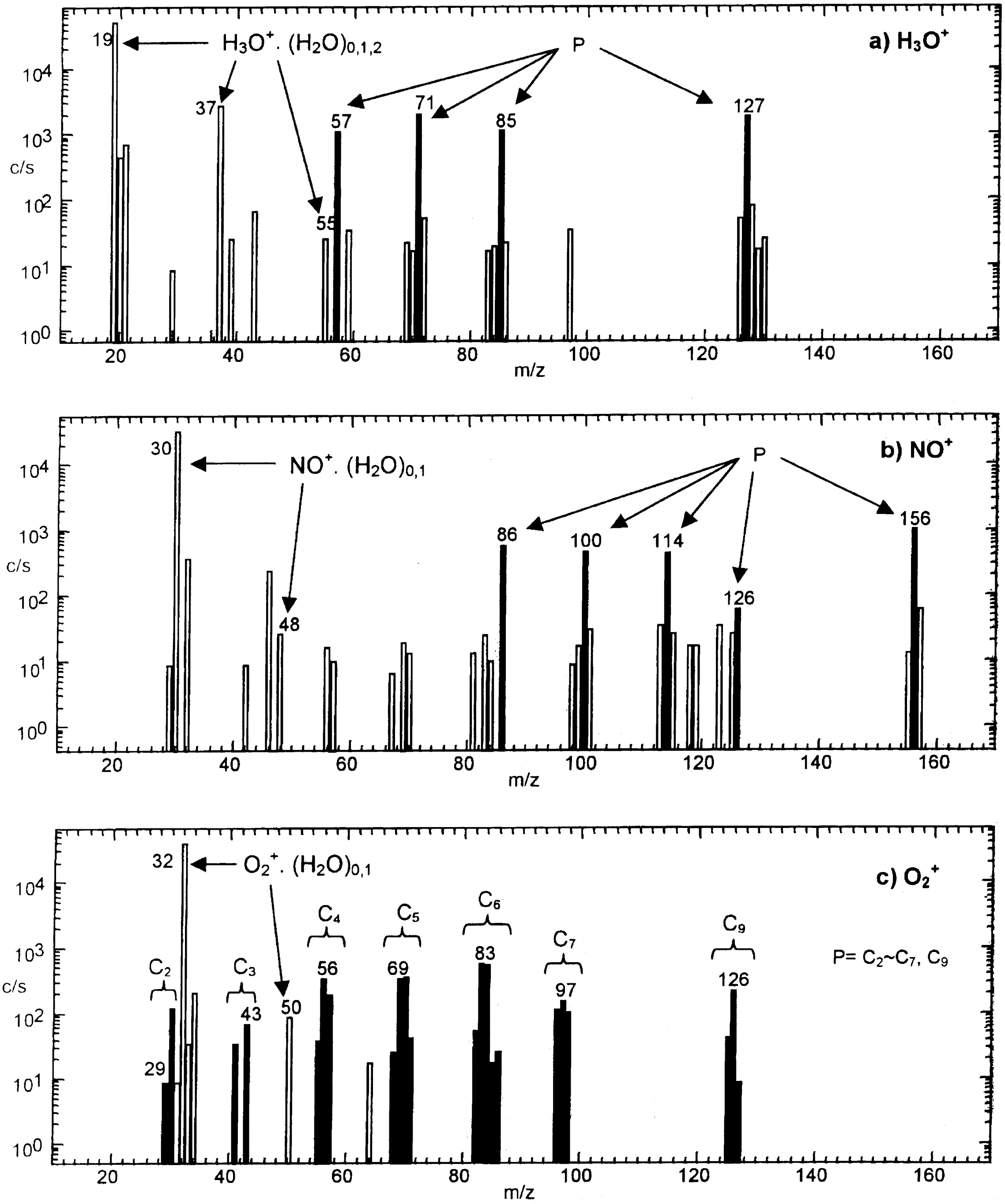

Fig. 2. Sample SIFT spectra obtained for: (a) H_3O^+, (b) NO^+ and (c) O_2^+ precursor ions reacting with 1-nonene (C_9H_{18}) as relatively dry air is also introduced into the helium carrier gas to quench any excited states of the precursor ions. As can be seen, small fractions of the hydrates of the precursor ions are formed, but these do not react with the 1-nonene. P indicates the individual product ions of the reactions. Note in the O_2^+ reactions that groups of ions are formed in the C_2 (very minor) to C_9 carbon chain length series, except C_8 (see also Fig. 5).

calculated from the count rates of these ions, see [35]) and the formation of $NO^+(H_2O)_{1,2}$ hydrates [36] ($O_2{}^+$ hydrates are not formed in significant fractions [33]). It is obviously important for meaningful SIFT-MS analyses to know if any of these hydrate ions react with the alkenes and also if any of the product ions of the reactions react with H_2O molecules, especially to form hydrates. This is an important investigation, because the exhaust gases from both the petrol and diesel engines are very humid (typically 10% water content [25]). We can find no evidence that the $H_3O^+(H_2O)_{1,2,3}$ hydrates and the $NO^+(H_2O)_{1,2}$ hydrates react with the alkenes. But a few of the product ions of the NO^+ reactions, i.e., the $RHNO^+$ ions (see the later discussion), undergo association reactions with H_2O molecules to form their hydrates, $RHNO^+{\cdot}H_2O$. Some of these hydrated ions can be seen in the spectra shown in Fig. 4b. The rate coefficients for these association reactions can be estimated by comparing the count rate ratios $[RHNO^+{\cdot}H_2O]/[RHNO^+]$ to the $[NO^+{\cdot}H_2O]/[NO^+]$ count rate ratio, the $NO^+{\cdot}H_2O$ hydrate ions being formed by the association reaction of NO^+ with H_2O in He, using the rate coefficient for the last reaction which has been measured to be $3.6\times10^{-29}\,cm^6/s$ [36]. This procedure has been discussed previously in a paper on the influence of humidity on SIFT-MS analysis [37] and used in our recent study of aldehyde reactions [23]. These estimated values are included in Table 3.

3. Results

3.1. General comments

The measured rate coefficients, k, for all the NO^+ and $O_2{}^+$ reactions are close to, but somewhat smaller than, the corresponding H_3O^+ reactions, in accordance with the larger reduced masses of the NO^+/alkene and $O_2{}^+$/alkene reactive systems. This is a clear indication that all the reactions in this study proceed at their collisional rates, i.e., that the $k = k_c$, their respective collisional rate coefficients. This simplifies the analysis of these compounds using SIFT-MS. It is also seen that the rate coefficients for the reactions of the 1-alkene isomers are slightly greater than those for the corresponding *trans*-2-alkene isomers, by virtue of the smaller permanent dipole moment of the latter isomers (see Table 1). As we will now see, the H_3O^+ reactions with both isomers of these alkenes all proceed via exothermic proton transfer which results in partial dissociation of the MH^+ product ions for the larger alkenes, M. However, the mechanisms of the NO^+ reactions are isomer specific, those involving the 1-alkenes proceed via $NO^+{\cdot}M$ production (three-body association) followed by partial dissociation of the nascent adduct ion to several product ions, into most of which NO is incorporated, whilst those involving the *trans*-2-alkene isomers proceed partially via charge transfer to give M^+ parent ions and partially via hydride ion (H^-) transfer to give $(M–H)^+$ ions. The $O_2{}^+$ reactions all proceed via charge transfer to give the parent M^+ radical ions together with multiple fragment ions.

3.2. H_3O^+ reactions

H_3O^+ ions undergo efficient (exothermic) proton transfer reactions with all these alkenes, M, included in this study. This contrasts with the corresponding alkane reactions in which proton transfer from H_3O^+ is endothermic and these reactions result in adduct ion formation, $H_3O^+{\cdot}M$ [20]. For both the pentene and hexene isomers the only observed products are the protonated parent molecules, MH^+, because it is apparent (using the available thermochemical data [38]) that dissociation channels (analogous to those for higher order alkenes), are too endothermic. Thus (in agreement with our previous result [20]), the 1-pentene reaction is simple:

$$H_3O^+ + CH_2{=}CHCH_2CH_2CH_3 \rightarrow C_5H_{11}{}^+ + H_2O \qquad (1)$$

The production of $C_2H_5{}^+$ ($+C_3H_6$) in this reaction would be endothermic by 113 kJ/mol. The corresponding reaction of *trans*-2-pentene is endothermic by 121 kJ/mol.

However, for both isomers of the longer chain alkenes, partial dissociation of the nascent MH^+ ions occurs and a simple picture appears. For both the heptene isomers, in addition to the MH^+ protonated parent molecule one additional product ion results, thus:

$$H_3O^+ + CH_2{=}CH(CH_2)_4CH_3 \rightarrow C_7H_{15}^+ + H_2O \tag{2a}$$

$$H_3O^+ + CH_2{=}CH(CH_2)_4CH_3 \rightarrow C_4H_9^+ + CH_2{=}CHCH_3 + H_2O \tag{2b}$$

It can be seen in Table 2, and also depicted in Fig. 3, that the branching ratios are somewhat different for the two isomeric heptene reactions, dissociation being somewhat more favoured in the 1-heptene reaction. Note that the double bond is retained in the neutral propene fragment. As can be seen in Table 2 and Fig. 3, that in the octene reactions there are two fragment ions produced, in the nonene reactions there are three fragment ions and in the 1-decene reaction there are four fragment ions:

$$H_3O^+ + CH_2{=}CH(CH_2)_7CH_3 \rightarrow C_{10}H_{21}^+ + H_2O \tag{3a}$$

$$H_3O^+ + CH_2{=}CH(CH_2)_7CH_3 \rightarrow C_7H_{15}^+(C_3H_6);\ C_6H_{13}^+(C_4H_8);\ C_5H_{11}^+(C_5H_{10});\ C_4H_9^+(C_6H_{12}) \tag{3b}$$

Clearly, fragmentation occurs at all points along the carbon chains in the $(MH^+)^*$ nascent cations, except that the double bond is retained in the neutral fragment. Hence, $C_4H_9^+$ is the smallest ion product in these protonation reactions. As can be seen in Table 2, there are only small differences in the branching ratios as between the two isomeric forms of each alkene. According to the available thermochemical data [38,39], all these fragmentation channels are remarkably close to thermoneutral; typically they are exothermic by less than 20 kJ/mol.

As mentioned previously, the $H_3O^+{\cdot}(H_2O)_{1,2,3}$ hydrate ions are formed from H_3O^+ when water vapour is present in the helium carrier gas. These hydrated ions may then behave as additional precursor ions, but we have observed on numerous occasions that the $H_3O^+{\cdot}(H_2O)_{1,2,3}$ ions are not very reactive with hydrocarbon molecules [40]. Thus, it is not surprising that hydrated hydrocarbon ions did not appear at significant levels in the product ion spectra in these experiments. This also means that the hydrocarbon product ions of these H_3O^+ reactions do not undergo three-body association with water molecules. This simplifies the analyses of these alkenes by SIFT-MS.

3.3. NO^+ reactions

NO^+ ions can undergo charge transfer reactions with molecules that have ionisation energies (IE)(M), lower than that of NO, which is 9.25 eV [41]. It is

Table 2
Product ions (and product neutrals in brackets) of the reactions of H_3O^+ with the 1- and *trans*-2-alkene isomers indicated with the product distributions in percent in brackets

Molecule	Product ions				
1-Pentene, C_5H_{10}	**$C_5H_{11}^+$ (100)**				
Trans-2-pentene	**$C_5H_{11}^+$ (100)**				
1-Hexene, C_6H_{12}	**$C_6H_{13}^+$ (100)**				
Trans-2-hexene	$C_6H_{13}^+$ (100)				
1-Heptene, C_7H_{14}	$C_4H_9^+$ (C_3H_6) (75)	**$C_7H_{15}^+$ (25)**			
Trans-2-heptene	$C_4H_9^+$ (C_3H_6) (65)	**$C_7H_{15}^+$ (35)**			
1-Octene, C_8H_{16}	$C_4H_9^+$ (C_4H_8) (35)	$C_5H_{11}^+$ (C_3H_6) (35)	**$C_8H_{17}^+$ (30)**		
Trans-2-octene	$C_4H_9^+$ (C_4H_8) (30)	$C_5H_{11}^+$ (C_3H_6) (35)	**$C_8H_{17}^+$ (35)**		
1-Nonene, C_9H_{18}	$C_4H_9^+$ (C_5H_{10}) (20)	$C_5H_{11}^+$ (C_4H_8) (30)	$C_6H_{13}^+$ (C_3H_6) (20)	**$C_9H_{19}^+$ (30)**	
Trans-2-nonene	$C_4H_9^+$ (C_5H_{10}) (20)	$C_5H_{11}^+$ (C_4H_8) (25)	$C_6H_{13}^+$ (C_3H_6) (15)	**$C_9H_{19}^+$ (40)**	
1-Decene, $C_{10}H_{20}$	$C_4H_9^+$ (C_6H_{12}) (10)	$C_5H_{11}^+$ (C_5H_{10}) (20)	$C_6H_{13}^+$ (C_4H_8) (15)	$C_7H_{15}^+$ (C_3H_6) (10)	**$C_{10}H_{21}^+$ (45)**

The product ions are ordered along the lines in increasing values of *m*/*z* to facilitate comparison with the product distribution as shown in Fig. 3. The protonated parent ions that partially fragment for the longer chain alkenes are indicated in bold.

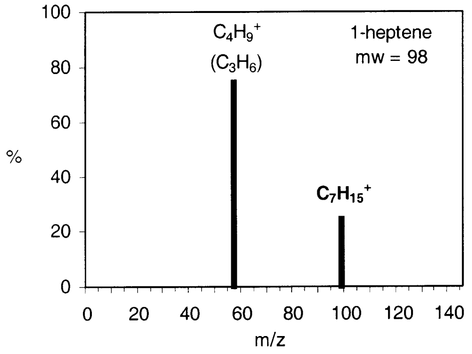
1-heptene
mw = 98
$C_4H_9^+$
(C_3H_6)
$C_7H_{15}^+$
%
m/z
0 20 40 60 80 100 120 140
0 20 40 60 80 100

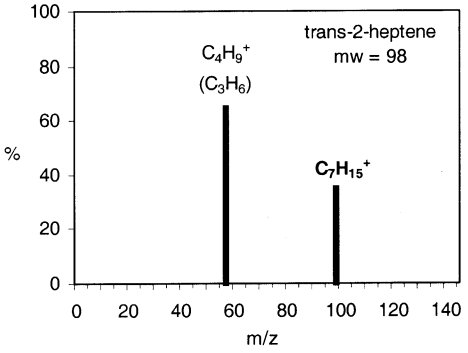
trans-2-heptene
mw = 98
$C_4H_9^+$
(C_3H_6)
$C_7H_{15}^+$
%
m/z
0 20 40 60 80 100 120 140
0 20 40 60 80 100

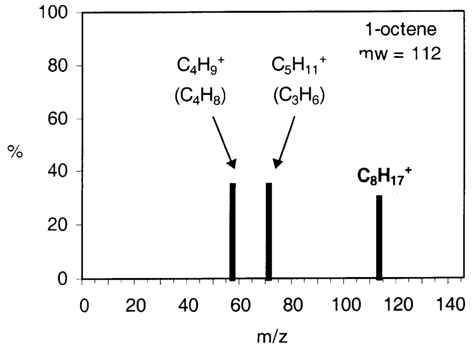
1-octene
mw = 112
$C_4H_9^+$
(C_4H_8)
$C_5H_{11}^+$
(C_3H_6)
$C_8H_{17}^+$
%
m/z
0 20 40 60 80 100 120 140
0 20 40 60 80 100

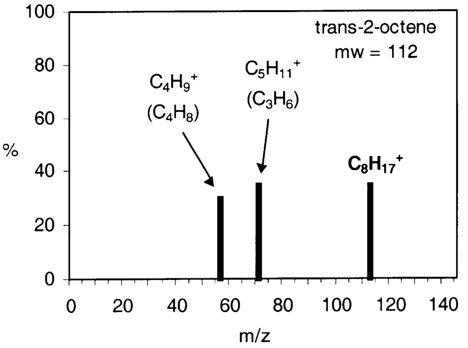
trans-2-octene
mw = 112
$C_4H_9^+$
(C_4H_8)
$C_5H_{11}^+$
(C_3H_6)
$C_8H_{17}^+$
%
m/z
0 20 40 60 80 100 120 140
0 20 40 60 80 100

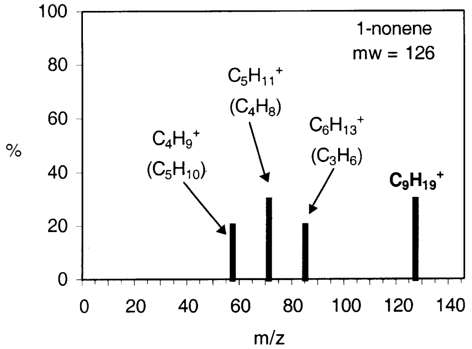
1-nonene
mw = 126
$C_5H_{11}^+$
(C_4H_8)
$C_4H_9^+$
(C_5H_{10})
$C_6H_{13}^+$
(C_3H_6)
$C_9H_{19}^+$
%
m/z
0 20 40 60 80 100 120 140
0 20 40 60 80 100

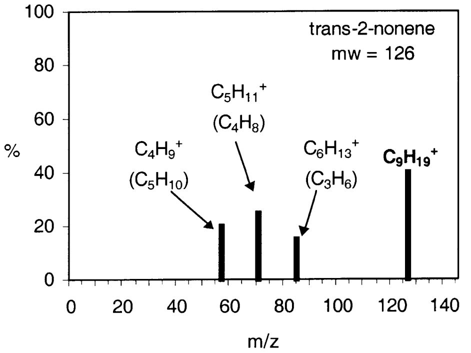
trans-2-nonene
mw = 126
$C_5H_{11}^+$
(C_4H_8)
$C_4H_9^+$
(C_5H_{10})
$C_6H_{13}^+$
(C_3H_6)
$C_9H_{19}^+$
%
m/z
0 20 40 60 80 100 120 140
0 20 40 60 80 100

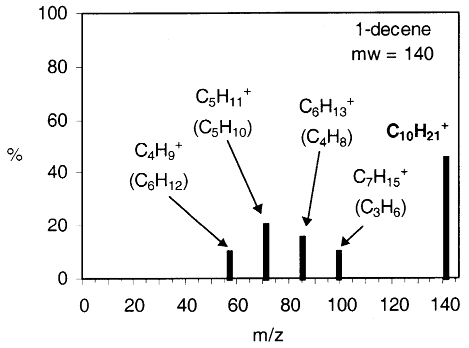
1-decene
mw = 140
$C_5H_{11}^+$
(C_5H_{10})
$C_6H_{13}^+$
(C_4H_8)
$C_{10}H_{21}^+$
$C_4H_9^+$
(C_6H_{12})
$C_7H_{15}^+$
(C_3H_6)
%
m/z
0 20 40 60 80 100 120 140
0 20 40 60 80 100

Table 3
Product ions of the reactions of NO^+ ions with the 1- and *trans*-2-alkene isomers with their percentages of each indicated in brackets

Molecule IE (eV)	Product ions			
1-Pentene, C_5H_{10} 9.49	CH_3HNO^+ (40)[a]	$C_4H_7^+$ (15)	$C_5H_9^+$ (10)	**$C_5H_9HNO^+$ (35)**[d]
Trans-2-pentene 9.04	$C_5H_9^+$ (50)	$C_5H_{10}^+$ (50)		
1-Hexene, C_6H_{12} 9.44	CH_3HNO^+ (15)[a]	$C_5H_9^+$ (10)	$C_3H_5HNO^+$ (10)[b]	$C_6H_{11}^+$ (5)
	$C_4H_7HNO^+$ (35)[c]	**$C_6H_{11}HNO^+$ (25)**[e]		
Trans-2-hexene 8.97	$C_6H_{11}^+$ (45)	$C_6H_{12}^+$ (55)		
1-Heptene, C_7H_{14} 9.34	CH_3HNO^+ (15)[a]	$C_3H_5HNO^+$ (5)[b]	$C_4H_7HNO^+$ (40)[c]	$C_7H_{13}^+$ (<5)
	$C_7H_{14}^+$ (<5)	$C_5H_9HNO^+$ (15)[d]	**$C_7H_{13}HNO^+$ (20)**	
Trans-2-heptene 8.84	$C_7H_{13}^+$ (40)	$C_7H_{14}^+$ (60)		
1-Octene, C_8H_{16} 9.43	CH_3HNO^+ (10)[a]	$C_4H_8^+$ (<5)	$C_3H_5HNO^+$ (<5)[b]	$C_4H_7HNO^+$ (25)[c]
	$C_5H_9HNO^+$ (20)[d]	$C_8H_{16}^+$ (<5)	$C_6H_{11}HNO^+$ (<5)[e]	**$C_8H_{15}HNO^+$ (30)**
Trans-2-octene 9.00	$C_8H_{15}^+$ (40)	$C_8H_{16}^+$ (60)		
1-Nonene, C_9H_{18} 9.42	$C_4H_7HNO^+$ (20)[c]	$C_5H_9HNO^+$ (20)[d]	$C_6H_{11}HNO^+$ (20)[e]	$C_9H_{18}^+$ (<5)
	$C_9H_{17}HNO^+$ (40)			
Trans-2-nonene 8.90	$C_5H_9HNO^+$ (5)[d]	$C_9H_{17}^+$ (30)	$C_9H_{18}^+$ (55)	**$C_9H_{17}HNO^+$ (10)**
1-Decene, $C_{10}H_{20}$ 9.42	$C_4H_7HNO^+$ (15)[c]	$C_5H_9HNO^+$ (15)[d]	$C_6H_{11}HNO^+$ (20)[e]	$C_7H_{13}HNO^+$ (<5)
	$C_{10}H_{20}^+$ (<5)	**$C_{10}H_{19}HNO^+$ (45)**		

Those ions containing NO are indicated as $RHNO^+$, where R is a radical (CH_3, C_3H_5, C_4H_7, etc.). The NO^+/alkene adduct ions that partially fragment are indicated in bold. Also indicated are estimates of the three-body association rate coefficients of some of the product ions with H_2O molecules pertaining to a helium pressure of 0.7 Torr with a small admixture of humid air (breath) and at 300 K. The ionisation energies are given below each alkene in electron volts, eV. The molecular formulae for the adduct ions do not necessarily represent their structures.

The three-body rate coefficient for the association reactions of water with the product ions are as follows: [a]CH_3HNO^+, 5×10^{-28} cm^6/s; [b]$C_3H_5HNO^+$, 4×10^{-28} cm^6/s; [c]$C_4H_7HNO^+$, 2×10^{-27} cm^6/s; [d]$C_5H_9HNO^+$, 4×10^{-28} cm^6/s; [e]$C_6H_{11}HNO^+$, 1×10^{-27} cm^6/s.

coincidental that the five *trans*-2-alkene isomers included in this study all have IE that are lower than IE(NO) (see Table 3) and charge transfer is indeed observed for all their reactions with NO^+. Conversely, the IE of all the 1-alkene isomers are greater than IE(NO) and in these reactions three-body association is observed followed by partial fragmentation of the $(NO^+{\cdot}M)^*$ nascent excited adduct ions. These surprisingly complex 1-alkene reactions are well exemplified by the 1-heptene reaction in which seven products are observed that represent a wide variety of concurrent processes:

$$\text{association}: \quad NO^+ + CH_2{=}CH(CH_2)_4CH_3(+He) \rightarrow C_7H_{13}HNO^+(+He) \qquad (4a)$$

$$\text{insertion}: \quad NO^+ + CH_2{=}CH(CH_2)_4CH_3 \rightarrow CH_3HNO^+ + C_6H_{10} \qquad (4b)$$

$$\text{insertion}: \quad NO^+ + CH_2{=}CH(CH_2)_4CH_3 \rightarrow C_3H_5HNO^+ + C_4H_8 \qquad (4c)$$

$$\text{insertion}: \quad NO^+ + CH_2{=}CH(CH_2)_4CH_3 \rightarrow C_4H_7HNO^+ + C_3H_6 \qquad (4d)$$

$$\text{insertion}: \quad NO^+ + CH_2{=}CH(CH_2)_4CH_3 \rightarrow C_5H_9HNO^+ + C_2H_4 \qquad (4e)$$

$$\text{H-transfer}: \quad NO^+ + CH_2{=}CH(CH_2)_4CH_3 \rightarrow C_7H_{13}^+ + HNO \qquad (4f)$$

Fig. 3. Percentage product ion distributions (%) for the reactions of H_3O^+ with the 1- and *trans*-2-alkenes indicated. The neutral fragment associated with each product ion (at mass-to-charge ratios, *m/z*) is given in brackets. The non-dissociated protonated parent molecule is indicated in bold type. Note that H_2O is a neutral product in each of these proton transfer reactions. Note also the increase in the number of products with the alkene chain length.

$$\text{charge transfer}: \quad NO^+ + CH_2{=}CH(CH_2)_4CH_3 \rightarrow C_7H_{14}{}^+ + NO \qquad (4g)$$

Note that the NO molecule is contained within the product ion in reactions (4b)–(4e) (these we designate insertion reactions). Reaction (4f) is a minor hydride ion transfer channel, this process being much more important in the reactions of the *trans*-2 isomers, as we discuss in the next section (see also Table 3). Reaction (4g) is a minor charge transfer channel that is somewhat endothermic according to the published IE of 1-heptene which is 9.34 eV [38]. However, this endothermicity ($9.34 - 9.25 = 0.09$ eV) is sufficiently small to allow a fraction of the reactants in the Maxwell–Boltzmann swarm to undergo charge transfer. This is also apparent in the 1-octene, 1-nonene and 1-decene reactions (see Table 3). Charge transfer is a major process in all the *trans*-2-alkene reactions (see below).

There is a tendency for the fraction of the $NO^+{\cdot}M$ adduct ions to increase with the chain length in these 1-alkene isomer reactions, as can be seen in Table 3 (although the 1-pentene reaction is apparently exceptional). Presumably, this is due to the greater numbers of vibrational degrees of freedom in the excited nascent adduct ions, $(NO^+{\cdot}M)^*$ that can store the bond energy and thus prolong their lifetimes against unimolecular decomposition to the observed fragment ions. Unfortunately, thermochemical data are not available with which to estimate the thermicities of these fragmentation (insertion) reactions, but clearly they must all be exothermic to proceed so efficiently under the thermalised conditions in the SIFT. The $RHNO^+$ product ions that are observed following dissociation (the R are the radicals CH_3, C_3H_5, C_4H_7, etc.) are like the similar saturated products ions $R'HNO^+$ (here, R′ are C_2H_5, C_3H_7, C_4H_9, etc.) that are observed in the reactions of the higher-order alkanes with NO^+ ions [20]. It is also worthy of note that the fraction of the $NO^+{\cdot}M$ adduct ions within the product distributions increases somewhat when breath (containing water vapour) is added to the carrier gas. This is presumably due to the greater efficiency of H_2O molecules (and also the breath CO_2 molecules that are introduced) in stabilising the nascent $(NO^+{\cdot}M)^*$ excited ions, which therefore reduces their degree of fragmentation.

The $RHNO^+$ product ions associate with H_2O molecules in three-body collisions with helium, forming the $RHNO^+{\cdot}H_2O$ hydrated ions. This can be seen very clearly in Fig. 4, which shows the product ion spectra for the NO^+/1-octene reaction with dry air introduced into the helium carrier gas (Fig. 4a) and then with humid air (breath) introduced into the carrier gas (Fig. 4b). Note the appearance of the hydrates in the presence of the water vapour. The estimated three-body rate coefficients for the formation of these hydrates are given in Table 3. The rate coefficients are comparable with those typical of the association reactions of protonated polar molecules with water [23,33]. Therefore, the H_2O molecules may be coupled via a hydrogen bond to the protonated N atom of the ion.

The reactions of NO^+ with the *trans*-2-alkene isomers proceed almost exclusively via parallel charge transfer and hydride ion transfer as, for example, in the *trans*-2-octene reaction:

$$NO^+ + CH_3CH{=}CH(CH_2)_4CH_3 \rightarrow C_8H_{16}{}^+ + NO \qquad (5a)$$

$$NO^+ + CH_3CH{=}CH(CH_2)_4CH_3 \rightarrow C_8H_{15}{}^+ + HNO \qquad (5b)$$

The charge transfer process is slightly favoured in these alkene reactions, as can be seen by a glance in Table 3. This obvious difference between these 1-alkene and *trans*-2-alkene reactions with NO^+ is useful in distinguishing between these isomeric forms. A similar distinction occurs between 1-butene and 2-butene according to the recent VT-SIFT study [26]. The *trans*-2-nonene reaction is exceptional amongst these *trans*-2 isomers in that a small association product and an additional fragmentation (insertion) channel are observed:

$$NO^+ + CH_3CH{=}CH(CH_2)_5CH_3 \rightarrow C_9H_{18}{}^+ + NO \qquad (6a)$$

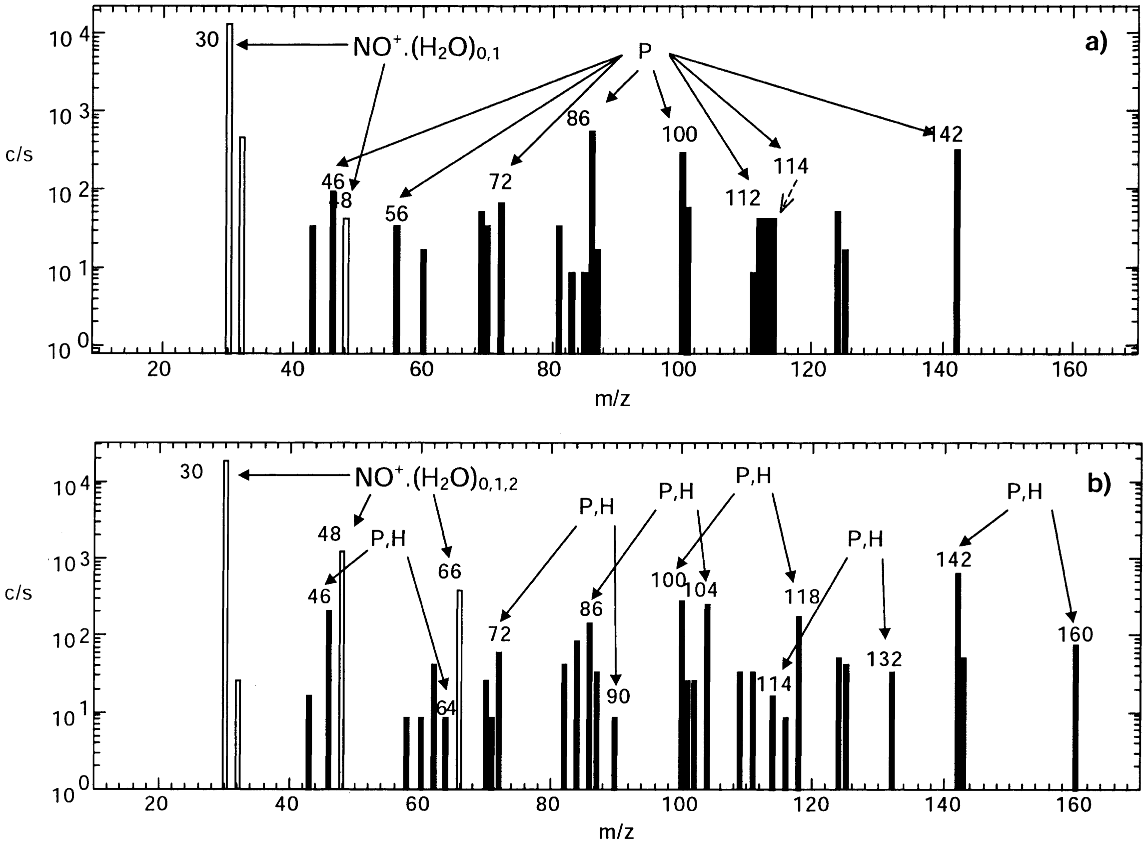

Fig. 4. SIFT spectra for the reaction of NO^+ precursor ions with 1-octene. Spectrum (a) was obtained as dry air was simultaneously introduced into the helium carrier gas (to quench any excited states). This indicates the primary products of the NO^+/1-octene reaction, as indicated by P. Spectrum (b) was obtained as a sample of breath rather than dry air at the same flow rate was introduced into the carrier gas. This indicates which of the product ions, P, form hydrates, which are indicated by H (see Table 3).

$$NO^+ + CH_3CH{=}CH(CH_2)_5CH_3 \rightarrow C_9H_{17}^+ + HNO \qquad (6b)$$

$$NO^+ + CH_3CH{=}CH(CH_2)_5CH_3 \rightarrow C_9H_{17}HNO^+ \qquad (6c)$$

$$NO^+ + CH_3CH{=}CH(CH_2)_5CH_3 \rightarrow C_5H_9HNO^+ + C_4H_8 \qquad (6d)$$

It appears that the rapid bimolecular reactions (6a) and (6b) are not so exothermic that they totally dominate the exit channels, thus allowing channels (6c) and (6d) to open.

3.4. O_2^+ reactions

O_2^+ ions undergo charge transfer reactions with all these alkenes producing parent M^+ ions and several fragment ions in the C_2 series to those in the parent cation series (C_{10} in the case of 1-decene), although the ions in the C_2 series are relatively rare. There are no major differences in the product spectra for the two isomeric forms of each alkene, but the major ion in these spectra are within adjacent series in the pentene and nonene reactions, as can be seen by inspection of Table 4. Examples of the spectra obtained are given in Fig. 5 for 1-hexene and the longer chain

Table 4
The spectral series of carbon atoms observed using O_2^+ precursor ions in the SIFT and the corresponding series observed following ionisation by 70 eV electrons of the alkenes indicated (data from [42])

Molecule	Ions observed		Most abundant ion	
	O_2^+, SIFT	EI	O_2^+, SIFT	EI
1-Pentene, C_5H_{10}	C_2–C_5	C_2–C_5	$C_3H_6^+$	$C_3H_6^+$
Trans-2-pentene	C_2–C_5	C_2–C_5	$C_4H_7^+$	$C_4H_7^+$
1-Hexene, C_6H_{12}	C_2–C_6	C_2–C_6	$C_4H_8^+$	$C_3H_5^+$
Trans-2-hexene	C_2–C_6	C_2–C_6	$C_4H_7^+$	$C_4H_7^+$
1-Heptene, C_7H_{14}	C_3–C_7	C_2–C_5, C_7	$C_4H_8^+$	$C_3H_5^+$
Trans-2-heptene	C_3–C_7	C_2–C_5, C_7	$C_4H_8^+$	$C_3H_5^+$
1-Octene, C_8H_{16}	C_3–C_6, C_8	C_2–C_6, C_8	$C_5H_{10}^+$	$C_3H_7^+$
Trans-2-octene	C_3–C_6, C_8	C_2–C_6, C_8	$C_5H_{10}^+$	$C_4H_7^+$
1-Nonene, C_9H_{18}	C_3–C_7, C_9	C_2–C_7, C_9	$C_6H_{11}^+$	$C_4H_8^+$
Trans-2-nonene	C_3–C_7, C_9	C_2–C_7, C_9	$C_5H_{10}^+$	$C_4H_7^+$
1-Decene, $C_{10}H_{20}$	C_4–C_8, C_{10}	C_2–C_8, C_{10}	$C_5H_9^+$	$C_3H_5^+$

The appearance of ions at lower *m*/*z* values in the EI series. Also given are the most abundant ions for each alkene, these usually being of lower *m*/*z* in the EI series.

trans-2-nonene. It is not useful to tabulate the detailed product distributions here, because of the many ions involved, which renders these O_2^+ reactions worthless for quantitative SIFT-MS analyses.

Fundamentally interesting are comparisons of the O_2^+ spectra with the corresponding electron ionisation (EI) spectra (obtained from the NIST database [42]), since the product ions originate from the same radical cation in different states of excitation. The direct comparisons for the 1-hexene and *trans*-2-nonene systems are presented in Fig. 5. It is clear that more complex fragmentation occurs following EI (C_2 and C_3 ions are more in evidence) and the major peaks are generally in one carbon series lower for the EI spectra than for the corresponding O_2^+ spectra. This can be seen in Fig. 5 and in Table 4 for all the alkenes included in this study. However, notice the absence of a C_8 series of ions in *trans*-2-nonene for ionisation by both O_2^+ and electrons (this C_8 series of ions is also absent in for 1-nonene isomer). It is also commonly the case that the majority ions in a particular series produced by O_2^+ ionisation are at *m*/*z* values 1 U higher than those for EI, e.g., at $m/z = 56$ and $m/z = 55$, respectively, in the C_4 series for 1-hexene:

$$O_2^+ + CH_2{=}CH(CH_2)_3CH_3 \rightarrow C_4H_8^+ + C_2H_4 + O_2 \tag{7a}$$

$$e^- \ (70\,\text{eV}) + CH_2{=}CH(CH_2)_3CH_3 \rightarrow C_4H_7^+ + C_2H_5 + 2e^- \tag{7b}$$

Tentatively, this can be interpreted thus: electron impact ionisation favours the rapid dissociation of the nascent excited parent cations before H-atom migration can occur [43], whilst the “softer” ionisation by the O_2^+ ions allows for the production of energetically allowed products that require H-atom motion within the excited ion. Generally speaking, the O_2^+ spectra are simpler than the EI spectra and contain fewer fragments and whilst the intensities of the ions signals are different, all the product ions of the O_2^+ reactions are present in the corresponding EI spectra.

Fig. 5. A comparison of the SIFT spectra obtained for the reaction of O_2^+ precursor ions with 1-hexene and *trans*-2-nonene with the relative abundances of the ions formed following the ionisation of these alkene isomers by 70 eV electrons (the EI spectra are taken from the NIST database [42]). Only the most abundant ion species in each carbon series (C_2–C_7, C_9) are indicated. Note the preponderance of ions in lower carbon series for the EI spectra compared to the O_2^+ spectra.

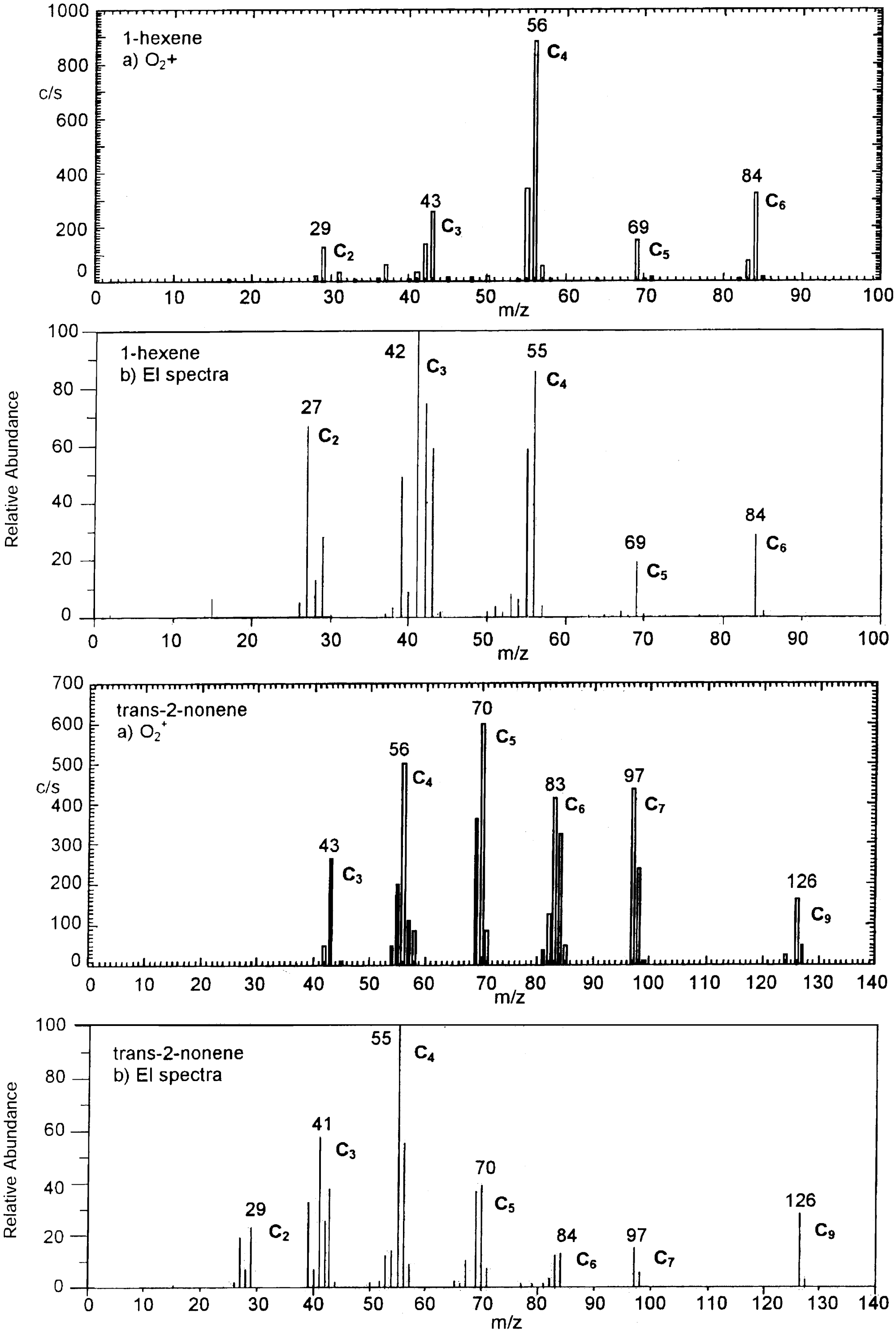
1-hexene
a) O_2^+
c/s
1000
800
600
400
200
0
56 C_4
43 C_3
29 C_2
69 C_5
84 C_6
0 10 20 30 40 50 60 70 80 90 100
m/z
Relative Abundance
1-hexene
b) EI spectra
100
80
60
40
20
0
42 C_3
55 C_4
27 C_2
69 C_5
84 C_6
0 10 20 30 40 50 60 70 80 90 100
m/z
trans-2-nonene
a) O_2^+
c/s
700
600
500
400
300
200
100
0
70 C_5
56 C_4
83 C_6
97 C_7
43 C_3
126 C_9
0 10 20 30 40 50 60 70 80 90 100 110 120 130 140
m/z
Relative Abundance
trans-2-nonene
b) EI spectra
100
80
60
40
20
0
55 C_4
41 C_3
70 C_5
29 C_2
84 C_6
97 C_7
126 C_9
0 10 20 30 40 50 60 70 80 90 100 110 120 130 140
m/z

4. Concluding remarks

Partial dissociation of the longer chain protonated alkenes (i.e., C_7 (heptene) chains and longer) formed in the H_3O^+ reactions occurs, which contrasts with the reactions of the analogous alkanes in which dissociation does not occur, but rather $H_3O^+\cdot M$ adducts form [20]. This complicates somewhat the analysis of these longer chain alkenes and alkanes using SIFT-MS. The reactions of the 1-alkenes with NO^+ are also complex in that multiple ions of the type $RHNO^+$ are formed, but the *trans*-2-alkene isomers react with NO^+ to produce M^+ and $(M–H)^+$ ions, which facilitates their analysis using SIFT-MS. The data obtained in this study is a valuable addition to the kinetics database required for SIFT-MS analysis. In common with their reactions with most organic species, $O_2{}^+$ ions are not useful for SIFT-MS analysis of alkanes and alkenes. However, $O_2{}^+$ is a valuable precursor ion for SIFT-MS analysis of small molecular species such as NO, NO_2 and NH_3 that do not dissociate in reaction with $O_2{}^+$ [4,33].

Acknowledgements

We gratefully acknowledge financial support by the Engineering and Physical Sciences Research Council, UK (grant reference GR/M89195/01) and also partial support by the Grant Agency of the Czech Republic (project numbers 203/00/0632 and 203/02/0737). We also thank Edward Hall for considerable technical assistance.

References

[1] D. Smith, P. Španěl, Int. Rev. Phys. Chem. 15 (1996) 231.
[2] D. Smith, P. Španěl, SIFT applications in mass spectrometry, in: J. Lindon, G. Trantner, J. Holmes (Eds.), Encyclopedia of Spectroscopy and Spectrometry, Mass Spectrometry, Academic Press, London, 1999, p. 2092.
[3] P. Španěl, D. Smith, Rapid Commun. Mass Spectrom. 13 (1999) 585.
[4] P. Španěl, D. Smith, T.A. Holland, W. Al Singari, J.B. Elder, Rapid Commun. Mass Spectrom. 13 (1999) 724.
[5] S. Davies, P. Španěl, D. Smith, Kidney Int. 52 (1997) 223.
[6] P. Španěl, D. Smith, T.A. Holland, W. Al Singari, J.B. Elder, Rapid Commun. Mass Spectrom. 13 (1999) 1354.
[7] D. Smith, P. Španěl, J.B. Jones, Bioresources Sci. Technol. 75 (2000) 27.
[8] R.J. Dewhurst, R.T. Evans, P. Španěl, D. Smith, Dairy Sci. 84 (2001) 1438.
[9] D. Smith, T. Wang, P. Španěl, Rapid Commun. Mass Spectrom. 16 (2002) 69.
[10] D. Smith, A.M. Diskin, Y. Ji, P. Španěl, Int. J. Mass Spectrom. 209 (2001) 81.
[11] P. Španěl, D. Smith, Rapid Commun. Mass Spectrom. 14 (2000) 1898.
[12] P. Španěl, D. Smith, J. Am. Mass Specrom. Soc. 12 (2001) 863.
[13] P. Španěl, D. Smith, Int. J. Mass Spectrom. Ion Processes 167/168 (1997) 375.
[14] P. Španěl, Y. Ji, D. Smith, Int. J. Mass Spectrom. Ion Processes 165/166 (1997) 25.
[15] P. Španěl, D. Smith, Int. J. Mass Spectrom. Ion Processes 172 (1998) 137.
[16] P. Španěl, D. Smith, Int. J. Mass Spectrom. Ion Processes 172 (1998) 239.
[17] P. Španěl, D. Smith, Int. J. Mass Spectrom. 176 (1998) 167.
[18] P. Španěl, D. Smith, Int. J. Mass Spectrom. 176 (1998) 203.
[19] P. Španěl, D. Smith, Int. J. Mass Spectrom. 185/186/187 (1999) 139.
[20] P. Španěl, D. Smith, Int. J. Mass Spectrom. 181 (1998) 1.
[21] P. Španěl, D. Smith, Int. J. Mass Spectrom. 184 (1999) 157.
[22] P. Španěl, D. Smith, Int. J. Mass Spectrom. 189 (1999) 213.
[23] P. Španěl, J.M. Van Doren, D. Smith, Int. J. Mass Spectrom. 213 (2002) 163.
[24] D. Smith, P. Cheng, P. Španěl, Rapid Commun. Mass Spectrom. 16 (2002) 1124.
[25] A.A. Abdel-Rahman, Int. J. Energy Res. 22 (1998) 483.
[26] A.J. Midey, S. Williams, A.A. Viggiano, J. Phys. Chem. A 105 (2001) 1574.
[27] D. Smith, N.G. Adams, Adv. Atom. Mol. Phys. 24 (1987) 1.
[28] E.P. Hunter, S.G. Lias, Proton affinity evaluation, in: W.G. Mallard, P.J. Linstrom (Eds.), NIST Chemistry WebBook, NIST Standard Reference Database Number 69, February 2000, National Institute of Standards and Technology, Gaithersburg, MD.
[29] G. Bouchoux, J.Y. Salpin, D. Leblanc, Int. J. Mass Spectrom. Ion Processes 153 (1996) 37.
[30] T. Su, W.J. Chesnavich, J. Chem. Phys. 76 (1982) 5183.
[31] D.R. Lide (Ed.), CRC Handbook of Chemistry and Physics, CRC, Boca Raton, 1991.
[32] N.G. Adams, D. Smith, in: A. Fontijn, M.A.A. Clyne (Eds.), Reactions of Small Transient Species Kinetics and Energetics, Academic, New York, 1983, Chapter 6, p. 311.
[33] Y. Ikezoe, S. Matsuoka, M. Takebe, A. Viggiano, Gas Phase Ion–Molecule Reaction Rate Constants Through 1986, Maruzen, Tokyo, 1987.
[34] J. Glosik, A.B. Rakshit, N.D. Twiddy, N.G. Adams, D. Smith, J. Phys. B 11 (1978) 3365.
[35] D. Smith, P. Španěl, Rapid Commun. Mass Spectrom. 15 (2001) 563.

[36] F.C. Fehsenfeld, M. Mosesman, E.E. Fergusson, J. Chem. Phys. 55 (1971) 2120.
[37] P. Španěl, D. Smith, Rapid Commun. Mass Spectrom. 14 (2000) 1898.
[38] S.G. Lias, J.E. Bartmess, J.F. Liebman, J.L. Holmes, R.D. Levin, W.G. Mallard, Ion energetics data, in: W.G. Mallard, P.J. Linstrom (Eds.), NIST Chemistry WebBook, NIST Standard Reference Database Number 69, February 2000, National Institute of Standards and Technology, Gaithersburg, MD.
[39] H.Y. Afeefy, J.F. Liebman, S.E. Stein, Neutral thermochemical data, in: W.G. Mallard, P.J. Linstrom (Eds.), NIST Chemistry WebBook, NIST Standard Reference Database Number 69, February 2000, National Institute of Standards and Technology, Gaithersburg, MD.
[40] P. Španěl, D. Smith, J. Phys. Chem. 99 (1995) 15551.
[41] S.G. Lias, Ionization energy evaluation, in: W.G. Mallard, P.J. Linstrom (Eds.), NIST Chemistry WebBook, NIST Standard Reference Database Number 69, February 2000, National Institute of Standards and Technology, Gaithersburg, MD.
[42] S.E. Stein (director) NIST Mass Spec Data Center (IR and Mass Spectra), in: W.G. Mallard, P.J. Linstrom (Eds.), NIST Chemistry WebBook, NIST Standard Reference Database Number 69, February 2000, National Institute of Standards and Technology, Gaithersburg, MD.
[43] F.W. McLafferty, F. Turecek, Interpretation of Mass Spectra, 4th Edition, University Science Books, Mill Valley, 1993.
[44] G. Espinosa, D. Yaffe, Y. Cohen, A. Arenas, F. Giralt, J. Chem. Inf. Comput. Sci. 40 (2000) 859.